

00188.26-02f

Potential Benefits of User-Preferred Descent Speed Profile

Tara Weidner
T. Golphar Davidson
Lance Birtcil



Seagull Technology, Inc.

Prepared for:

National Aeronautics and Space Administration
Ames Research Center, Moffett Field, CA 94035

Under:

SRC Subcontract No. 99-0249, Task Order No. RTO-26 1266-090

NASA Prime Contract No. NAS2-98005

Seagull Project No. C188.26

December 2000

Acknowledgment

This research was performed by Seagull Technology, Inc., as a subcontract to System Resources Corporation (SRC) for the NASA Ames Research Center's Advanced Air Transportation Technologies (AATT) Program. The authors appreciate the discussions, technical direction, and program management of Steve Green and Rich Coppenbarger within the En Route Operations branch of NASA Ames Research Center. This contract is the culmination of previous work begun under the FMS-ATM Next Generation (FANG) program for the FAA Aeronautical Data Link program, led by Bill Blake and later Mike Hawthorne, and now encompassed by the work of RTCA SC194 Working Group 2. The research was primarily performed by the authors under the program management of Tara Weidner. The previous work was led by John Sorensen of Seagull Technology.

Table of Contents

INTRODUCTION.....	1
1. ASSUMED OPERATIONAL CASES	3
Case 1. CTAS EDA Baseline.....	3
Case 2. User-Preferred (FMS) Speed Profile.....	4
2. ANALYSIS	5
2.1. Arrival Metering Delay	5
Airport Traffic Schedule	5
Metered Arrival Delays.....	6
2.2. CTAS EDA & User-Preferred Speed Strategy	7
Mach/CAS Descents	8
CTAS EDA and User-Preferred Speed Control Methods.....	10
2.3. Speed Strategy Fuelburn.....	12
High-Fidelity Aircraft Performance Simulations.....	12
Fuel Scale Factors	17
3. POTENTIAL EDX FUEL BENEFITS.....	19
1996 NAS-wide Annual Savings	19
CONCLUSIONS AND RECOMMENDATIONS.....	25
APPENDIX A FUEL SCALE FACTOR ASSUMPTIONS.....	28
ACRONYMS	30
REFERENCES.....	34

List of Figures

Figure 1. Dallas-Fort Worth International Airport.....	2
Figure 2. Plan and Profile View of DFW Study Day Operations	6
Figure 3. Air Traffic Controller Use of TMA to Schedule Aircraft	6
Figure 4. TMA Metered Arrival Delays.....	7
Figure 5. Simulated Five-Segment Descent Profile.....	8
Figure 6. Mach, CAS and TAS Relationships as a Function of Altitude	9
Figure 7. Altitude, Mach, CAS, Range and Time for a Typical Mach/CAS Descent	10
Figure 8. Photographs of MD-80 and B-747 Aircraft.....	12
Figure 9. Time-to-Fly and Fuelburn Contours by Mach/CAS Descent Speed Pairs	13
Figure 10a. Mach/CAS Plots for the MD-80 Aircraft.....	14
Figure 10b. Mach/CAS Plots for the B-747 Aircraft.....	15
Figure 11. Fuel/RTA Plot for MD-80 and B-747 Aircraft.....	15
Figure 12. Fuelburn vs. Delay Plots for MD-80 and B-747 Aircraft	16
Figure 13. Fuel Savings per Operation.....	19
Figure 14. User-Preferred Descent Speed Profile Annual Savings.....	23

List of Tables

Table 1. DFW Scheduling Criteria	7
Table 2. Assumed Nominal (Undelayed) Descent Trajectory	16
Table 3. DFW Fuel Benefits	19
Table 4. DFW Daily Simulation Interruption Rates and Costs	20
Table 5. Rush Arrival Rate Criteria.....	20
Table 6. User-Preferred Descent Speed Profile Annual Savings	22
Table A-1. Fuel Scale Factor Assumptions	28

Introduction

Coordinated research and development programs by the National Aeronautics and Space Administration (NASA), Federal Aviation Administration (FAA), and aviation industry are defining concepts for improving future air traffic operations. These programs include concepts for advance Air Traffic Management (ATM) automation and its integration, using data link communications, with advance flight management systems (FMSs).

The Center-TRACON Automation System (CTAS) [1], is an ATM automation program under development by NASA. One proposed CTAS tool is the En Route/Descent Advisor (EDA) [2], which will manage traffic within and between Air Route Traffic Control Centers (Centers) to facilitate free flight. EDA aims to reduce and improve the efficiency of deviations from the user's preferred trajectory. By generating accurate, fuel-efficient clearance advisories for the merging, sequencing, and separation of high-density en route traffic.

One of the future enhancements of CTAS is to integrate computations and information within the CTAS ground system with those of the FMS through data link [3]. Past and ongoing NASA and FAA research [4-12] has examined this concept with the objective of trajectory negotiation between CTAS EDA and the FMS. One potential advantage of CTAS-FMS negotiation is the potential to generate more user-preferred fuel-efficient approach trajectories than CTAS EDA operating alone because the FMS would have better internal knowledge of aircraft intent and performance, as well as local wind and air temperature.

This study was designed to determine the rough order of magnitude (ROM) fuel savings benefit available to aircraft with the implementation of CTAS-FMS descent profile negotiation. The magnitude of the potential fuel savings from CTAS-FMS trajectory negotiation will help determine if these savings are sufficient to warrant development of the infrastructure to implement trajectory negotiation capabilities. This study addresses the potential flight efficiency benefits of CTAS-FMS speed profile negotiation. The fuel savings of the user-preferred FMS trajectory is compared to CTAS EDA-calculated descent speed profiles over a typical day traffic scenario at a single airport. Typical-day simulation results are tabulated and extrapolated to annual and NAS-wide benefit estimates. Dallas-Fort Worth International Airport (DFW) traffic data was used to determine the per flight arrival delays over a typical day. A combination of high-fidelity aircraft performance models and scaling factors were used to calculate fleet-wide fuelburn savings for the day's delayed arrivals. The DFW arrival delays [13-14] and per operation fuel savings [15-17] were developed in previous studies.

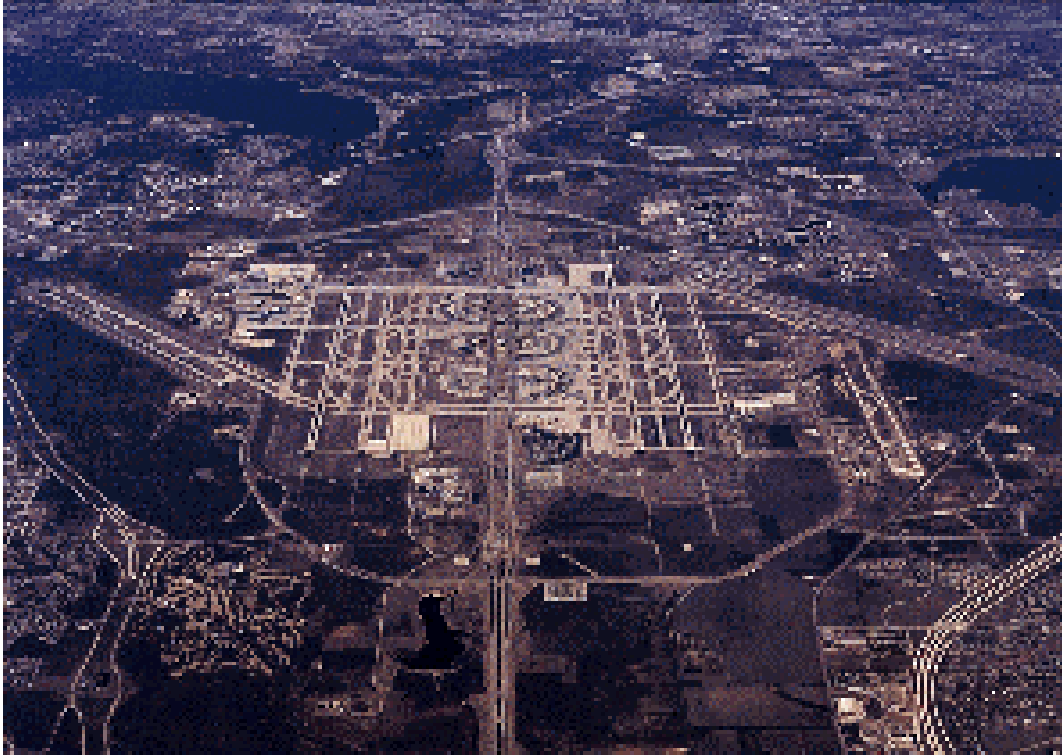


**Figure 1. Dallas-Fort Worth International Airport
(photo courtesy of NASA Ames Research Center)**

In the analysis, a hypothetical Required Time-of-Arrival (RTA)-capable FMS is represented by an aircraft following an approach trajectory steered to a fuel-optimal time-of-arrival (metering conformance) strategy. It is assumed that CTAS EDA and the hypothetical FMS share accurate estimates of meteorological conditions (wind, temperature) and aircraft weight through the use of data link. Many efforts are pursuing such passive data exchange [4-12] including a planned joint NASA/FAA field test scheduled for fall 2000 [9]. External factors affecting the execution of the advisories, such as traffic or airspace constraints, are not considered in this investigation.

The remainder of this report discusses background information, analyses and benefit estimates for descent speed intent negotiation operations. Chapter 1 describes the assumed operational cases; CTAS EDA Baseline and EDA augmented with user-preferred FMS speed intent data exchange. Chapter 2 documents the analysis methods and assumptions, including the modeled CTAS EDA and user-preferred FMS speed strategies. Aircraft simulation and modeling used to analyze these strategies are also addressed. The potential benefit fuel-efficiency estimates from these analyses are presented in Chapter 3, with conclusions and recommendations summarized in Chapter 4.

1. Assumed Operational Cases

The following en route operations cases describe a system baseline, reflecting Center TRACON Automation System (CTAS) En Route/Descent Advisor (EDA) capabilities, and an advanced system enhanced with en route data exchange of user-preferred FMS descent speed schedule. The FMS case is shown to lead to more efficient speed control delay advisories in addition to the benefit of honoring user preferences. The fuel efficiency results as the employed delay strategy utilizes the more accurate FMS trajectory optimization algorithms in generating its aircraft-specific speed profile.

Both modeled cases are assumed to employ the CTAS Traffic Management Advisor (TMA) tool to schedule arriving aircraft and identify per aircraft delays, necessary to meet downstream flow-rate restrictions. Additionally, the analysis only assesses speed control delay absorption, one of several methods used to delay aircraft. Other methods include changes in altitude and vectoring. Because this analysis focuses only on the speed control strategy, only a portion of the required arrival delays are absorbed. Under the speed control method, the flight crew may change the aircraft speed during cruise, during descent or both. In this investigation both the cruise and descent speeds are available as means of speed control; therefore, the aircraft may alter its cruise speed as well as its descent speed in order to meet its time constraint, at a constant range-to-fly. Other assumptions are identified below:

Case 1. CTAS EDA Baseline

Case 1 operations include the capabilities of both the CTAS TMA and EDA tools. This includes TMA arrival scheduling and EDA high-fidelity trajectory modeling to predict future aircraft positions and calculate metering conformance maneuver advisories. The EDA-generated maneuver advisories assist controllers in formulating and executing a traffic delay strategy to meet the TMA schedule, allowing the controller to quickly and accurately assess the impact of various approaches. In generating speed advisories for aircraft metering fix crossing, EDA uses the nominal CTAS model of an aircraft's aerodynamic and propulsion performance characteristics, estimated weight, and wind and air temperature forecasts to calculate required cruise and descent speeds. For this study, aircraft weight and meteorological forecasts (wind and temperature) are shared via CTAS-FMS data exchange. EDA [2] initially attempts to employ fuel efficient speed control to delay the aircraft. If speed control alone is not sufficient, a combination of altitude/speed adjustments are used and an optimal speed/altitude combination is advised, difficult to calculate without EDA data and computational assistance. Finally, vectoring, the least precise and least efficient strategy is reserved for large delays, and precise "turn-back" advisories are provided. As References [13-14] show, EDA-calculated advisories significantly increase the use of speed control as a delay strategy, over systems with controller-developed delay strategies.

Case 2. User-Preferred (FMS) Speed Profile

Case 2 operations address the same TMA-based arrival delays as in the baseline case, but here the EDA-speed advisory is assumed to be replaced with a user-preferred speed profile, downlinked from the FMS in real-time. Initially a Required Time-of-Arrival (RTA) restriction, assumed to be the TMA-calculated metering fix Scheduled Time-of-Arrival (STA), is uplinked to the aircraft. The flight crew then uses the on-board FMS RTA capability to generate its optimum speed profile to meet the metering fix crossing time restriction. This Mach/CAS descent speed profile is downlinked as an user-preferred trajectory. Full equipage of FMS trajectory optimization and RTA guidance capabilities is assumed.

2. Analysis

To assess the potential fuel benefits of user-preferred descent speed, the fuel efficiency of a CTAS-FMS speed profile negotiation case was compared to a CTAS EDA Baseline case, as described in the previous chapter. The following steps were employed. The specific methodology and results of each step are discussed in the remainder of this chapter.

- **Arrival Metering Delay** – Aircraft-specific metered arrival delays for a typical daily DFW traffic scenario are calculated.
- **Speed Strategy** – CTAS EDA and user-preferred FMS speed control strategies are defined.
- **Speed Strategy Fuelburn** – Fuel consumption under CTAS EDA and user-preferred FMS speed control strategies, at various delay values, are identified
- **Fuel Benefits** - Potential fleet-wide fuelburn savings from the DFW daily simulation are extrapolated to annual and NAS-wide deployment benefits

2.1. Arrival Metering Delay

The benefits analysis begins by defining an en route set of air-traffic “demand” trajectories for a typical day within a block of en route airspace. The DFW en route airspace traffic scenario comprises a set of four-dimensional (4D) “undelayed” trajectories, representing what each flight would do if left alone to fly the user’s preferred trajectory. These trajectories define the arrival congestion traffic scenario to be evaluated.

The traffic scenario is analyzed to determine the natural sequence and level of congestion for arrivals at DFW, the target airport. Arrival metering conformance operations are modeled and Scheduled times-of-arrival (STAs) are assigned for each arrival flight. These scheduled crossing times resolve downstream airport flow rate restrictions. A set of arrival flight delays is defined, as necessary to meet the metering fix STAs.

Airport Traffic Schedule

In this study the Fort Worth Air Route Traffic Control Center (ZFW) airspace was analyzed, including arrival, departure, and overflight traffic operations between 40 and 250 nautical miles (nm), at or above 10,000 ft from Dallas-Fort Worth International Airport (DFW). Enhanced Traffic Management System (ETMS)-based flight trajectories for a typical day (Friday, June 14, 1996) were used to generate nominal trajectories for approximately 2,500 DFW arrivals and departures [18]. Sample-day operations (arrival, departure and overflight) are illustrated in plan and profile view in Figure 2.

Standard departure and arrival routes, commonly known as Standard Instrument Departure (SID) and Standard Terminal Arrival Routes (STAR), are published procedures to aid in the coordination and routing of air traffic between Center and TRACON airspace. Aircraft typically follow SIDs and STARs to/from major airports. These routes are characterized by specific waypoints, headings, speeds, and other parameters. The modeled undelayed ZFW trajectories followed DFW SID and STAR routings, as shown in Figure 2.

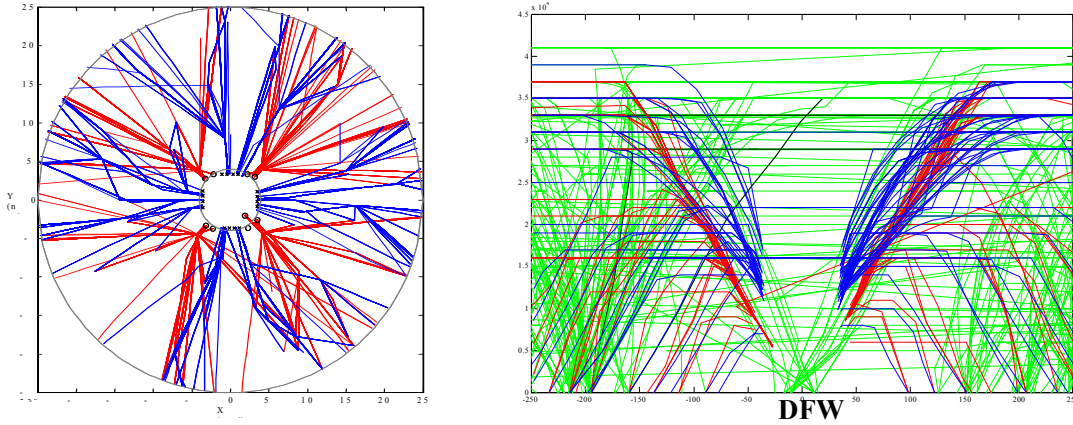
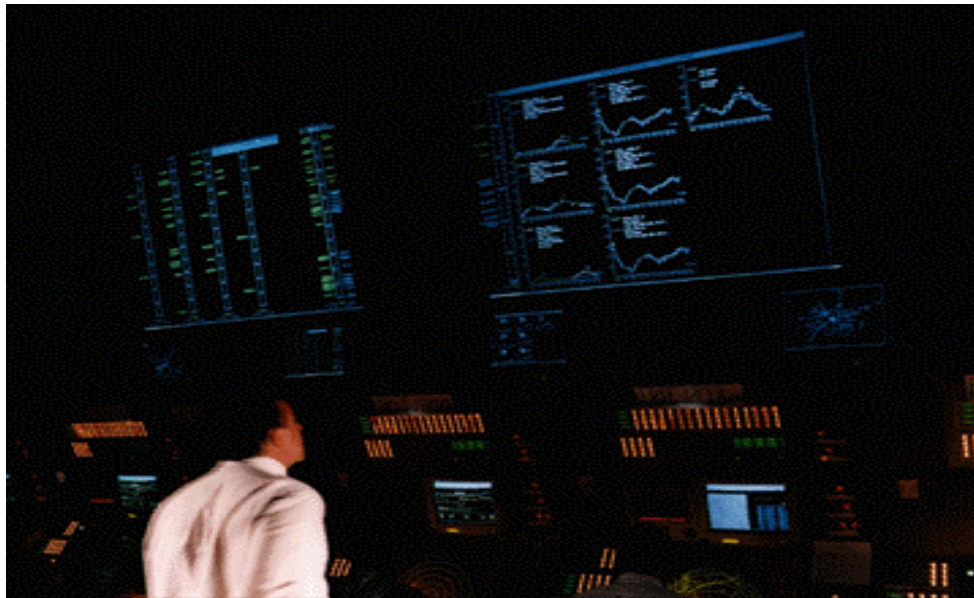


Figure 2. Plan and Profile View of DFW Study Day Operations

Metered Arrival Delays

During peak periods controllers meter arrival flights to meet airport capacity restrictions. Both cases under study are assumed to employ the CTAS Traffic Manager Advisor (TMA) for scheduling arrival aircraft into the TRACON, as shown in Figure 3.



**Figure 3. Air Traffic Controller Use of TMA to Schedule Aircraft
(photo courtesy of NASA Ames Research Center)**

TMA is designed to improve the flow of arrival traffic in the extended terminal airspace in compliance with air traffic rules [19]. TMA creates an optimum time-based arrival schedule for an airport complex and establishes scheduled times-of-arrival (STAs) at TRACON-boundary meter fixes to control the flow into the TRACON airspace, using very accurate cruise and descent trajectories based on high-fidelity aircraft performance models, wind aloft predictions, and flight plans. The TMA schedule is continually updated from radar returns flight data from the ARTCC Host computer system in response to changing events, until an aircraft's metering-fix Estimated Time-of-Arrival

(ETA) is within 19 minutes (the “freeze horizon”), at which point the aircraft's Scheduled time-of-arrival (STA) is frozen. TMA STAs are distributed to each en route sector managing arrival traffic. The STAs and TMA estimates of delay to be absorbed are displayed directly on the controller’s Display System Replacement (DSR) in an alphanumeric meter list.

For this effort, a simplified model of TMA metering was developed to estimate metering delays for each DFW arrival operation. Meter-fix scheduled times-of-arrival (STAs) at the TRACON boundary, and associated delays, were based on maximum TRACON entry rates and minimum inter-arrival fix separations, as shown in Table 1. Figure 4 shows a distribution of the arrival delays required to meet the Table 1 constraints over the course of the sample day. Speed control delay methods, evaluated in this effort, can only absorb 1-2 minutes of delay. Thus, delays in excess of the maximum speed control delay were ignored for this study.

Table 1. DFW Scheduling Criteria

Scheduling Criteria	Assumed Value
Minimum Arrival Meter-Fix In-Trail Separation	5.50 nm
Maximum TRACON Arrival Rate (4 Arrival Runways)	150 ac/hr

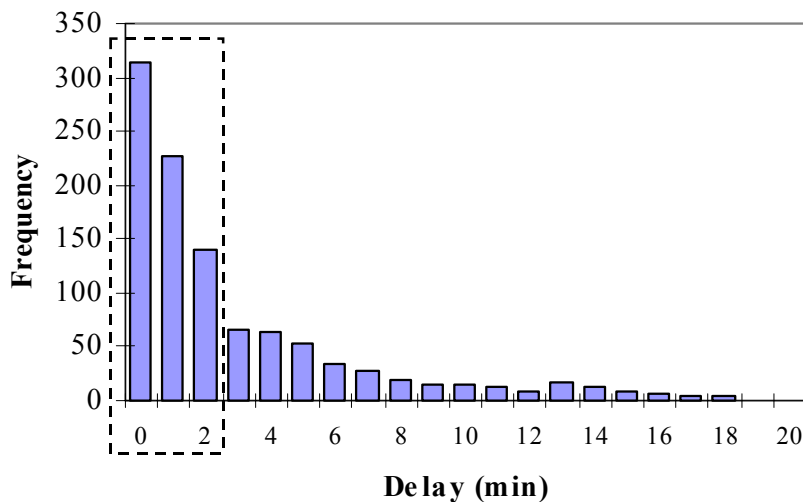


Figure 4. TMA Metered Arrival Delays

2.2. CTAS EDA & User-Preferred Speed Strategy

The particular speed strategies used to absorb the arrival metering delay differ between user (FMS) and ATM (CTAS EDA) strategies. Both are assumed to employ the standard Mach/CAS descent speed profile and top-of-descent (TOD) location. The Mach/CAS approach trajectory and the particular user-preferred FMS and CTAS EDA strategies employed in this study are discussed below.

Mach/CAS Descents

In the analysis, a nominal aircraft Mach/CAS approach trajectory was assumed, representing a typical descent from the cruise altitude to the metering fix altitude. Mach/CAS descents employ a descent speed profile characterized by a constant Mach segment followed by a constant calibrated airspeed (CAS) segment, performed at idle thrust for maximum fuel efficiency. Mach/CAS descent schedules are typically described in aircraft operating manuals. The Mach/CAS speeds can be adjusted to yield optimum fuel efficiency, time efficiency, or a combination of the two. Airline policies may recommend selected Mach/CAS schedules to suit their specific operational and economic conditions.

The assumed descent trajectory is divided into five stages, as shown in Figure 5. As shown, the modeled descent begins its trajectory in cruise (35,000 ft) at a constant cruise Mach speed and descends at the TOD, using the Mach/CAS schedule (segments 3 and 4) to the bottom-of-descent metering fix altitude and speed. The aircraft is assumed to reach the metering fix crossing speed (250 kt \pm kt) at the metering fix crossing altitude (10,000 ft \pm 20 ft) at the end of the simulation range (\pm 0.1 nm).

Speed adjustments may be required prior to the TOD (segment 2) or at the bottom of descent (segment 5). Figure 6 illustrates how Mach and CAS and true airspeed (TAS) vary with altitude under standard day conditions. Given a Mach/CAS speed combination, the figure shows that there generally exists an altitude at which the Mach number and CAS equate to the same true airspeed (TAS). In a descent, this is the transition altitude where speed control switches from maintaining constant Mach to maintaining constant CAS. Figure 6 can also identify constraints of the Mach/CAS combinations. Note that the descents may not have a constant Mach descent segment if the descent TAS (segment 4) is less than or equal to the cruise TAS (segment 2).

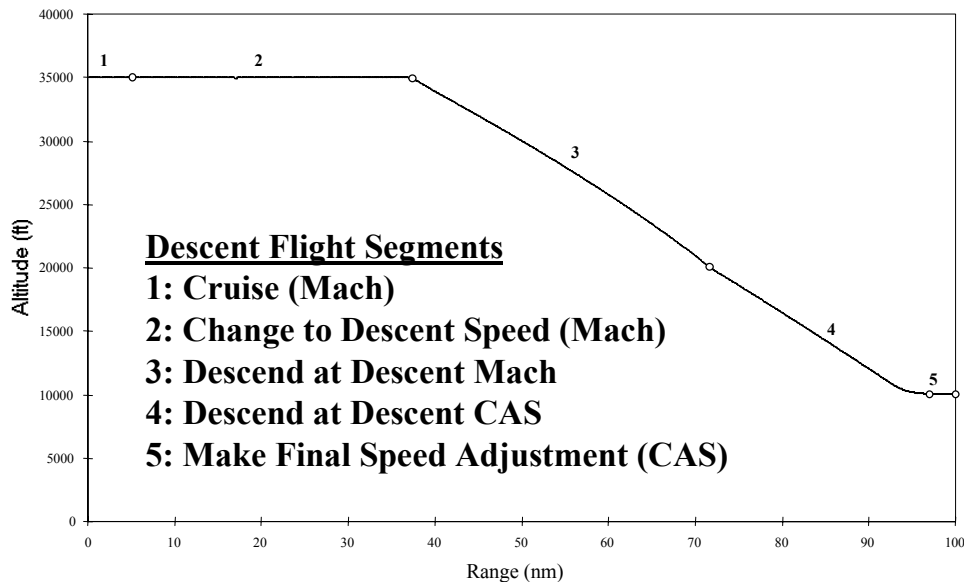


Figure 5. Simulated Five-Segment Descent Profile

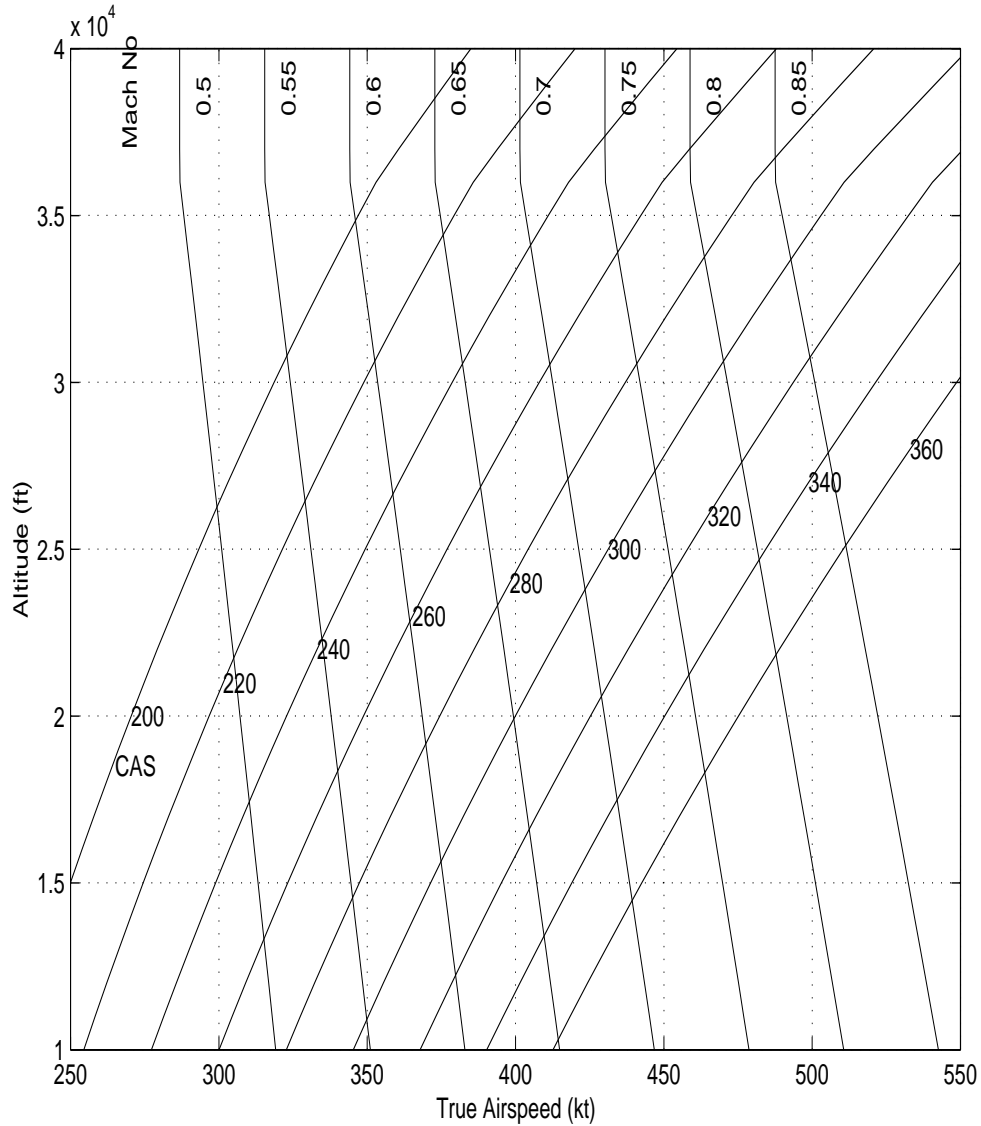


Figure 6. Mach, CAS and TAS Relationships as a Function of Altitude

The simulated speed-control process for a representative Mach/CAS schedule of 0.65/280 is illustrated in Figure 7. The aircraft, cruising at Mach 0.82 and 35,000 ft, immediately decelerates to Mach 0.65, with the speed change (Segment 1) complete at a range of about 10 nm. The aircraft maintains this cruise speed until the TOD, at about 34 nm (Segment 2). The aircraft then begins its descent at constant Mach 0.65 to a range of about 61 nm (Segment 3). During the constant-Mach portion of the descent, the CAS gradually increases from 215 kt to 280 kt. At about 23,500 ft, Mach 0.65 is equivalent to 280 kt CAS, and the aircraft switches to descend at constant CAS (Segment 4). At 95 nm, the aircraft has reached 10,000 ft, where it levels-off and decelerates to 250 kt CAS (Segment 5).

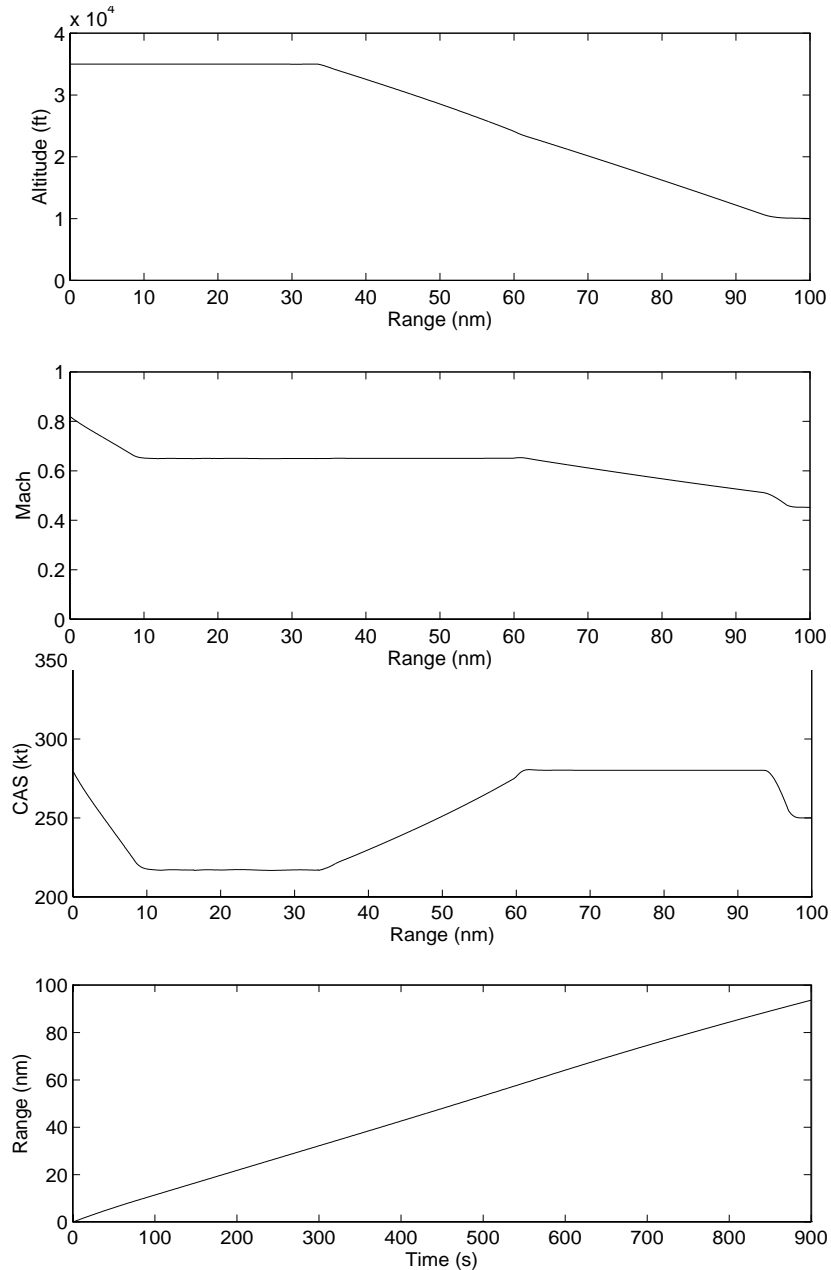


Figure 7. Altitude, Mach, CAS, Range and Time for a Typical Mach/CAS Descent

CTAS EDA and User-Preferred Speed Control Methods

Each strategy under study aims to predict an efficient descent speed and altitude profile to meet a metering fix crossing time, requiring delay absorption from the nominal trajectory. Both cruise speed and descent speed can be adjusted to meet the required time-of-arrival.

In both cases, it is assumed that implementation of each of these strategies makes use of common meteorological (wind, temperature) forecasts and aircraft weight data. These parameters are assumed to be error-free and shared by CTAS EDA and the FMS through data exchange. It is further assumed that the trajectories computed with each time-of-arrival control strategy may be executed without conflict, as conflict detection or resolution was not considered.

Unlike the modeled user-preferred FMS strategy, the current CTAS EDA strategies have been developed with consideration of operational constraints. The user-preferred FMS strategy selects Mach/CAS descent speed pairs without concern about operational issues such as multiple speed changes during a single approach trajectory. As an example, the fuel-optimal strategy may select a descent Mach that is significantly different from the cruise speed, requiring the aircraft to change speed before the top of descent. It may be operationally impractical to impose such an additional speed change before descent.

CTAS EDA Descents

Approach profiles generated by the CTAS EDA are similar to the nominal approach profile illustrated in Figure 5, characterized by an initial cruise speed (Segment 1), a second cruise speed (Segment 2), a constant descent Mach (Segment 3), a constant descent CAS (Segment 4), and finally, a transition to the metering fix airspeed (segment 5). When determining the speed profile required for a given metering fix RTA, the EDA first evaluates the time-of-arrival of the aircraft at the metering fix using a default descent profile. The default descent profile is specified by the airspeed of the constant CAS descent segment (Segment 4), and can be changed within the CTAS logic. The default cruise speed is the current (Segment 1) cruise speed. If the time-of-arrival calculated using the default profile requires delay, EDA shortens the descent duration using one of three speed strategies. In a special case, where the descent CAS selected by the EDA is the same as the cruise CAS, the aircraft does not change speed. In this case, the speed-change segment (Segment 2) and the constant Mach segment (Segment 3) are omitted from the approach trajectory. The three CTAS EDA strategies include: Cruise-Equals-Descent (C=D), Cruise-Then-Descent (C→D), Descent-Then-Cruise (D→C). Only the C=D strategy will be used for this analysis. Under the C=D strategy, if the aircraft must reduce its speed to meet a metering fix crossing time, the descent speed is set to essentially “balance” cruise and descent CAS speeds. The higher of cruise/descent CAS is initially decremented until both speeds are equal. Then each speed is alternately decremented. This strategy attempts to reduce the need for significant speed changes between cruise and descent by bringing the cruise and descent speeds closer. Although actual controller techniques may not be so precise, this approach conservatively represents controller actions.

User-Preferred FMS (Fuel-Optimal) Descents

Given a metering fix RTA up-linked from CTAS, the FMS computes a fuel-efficient Mach/CAS descent profile. User-preferred FMS-computed descents are optimistically represented in this study as the fuel-optimal descent speed and altitude profile. This assumes that a RTA-capable FMS would be able to calculate the minimum fuel descent to meet the metering fix RTA. An actual FMS is likely to achieve similar, but less fuel-efficient results.

The descent profile in this model is also similar to the nominal approach profile illustrated in Figure 5. The trajectory begins with a fixed cruise Mach (Segment 1). Immediately after the start of the trajectory, the aircraft changes speed to a new Mach number that is held for the remainder of the cruise (Segment 2) and the beginning of the descent profile (Segment 3). When this Mach number intersects the specified descent CAS, a transition is made to the constant CAS, which is held until the metering fix crossing altitude (Segment 4). At the metering fix crossing altitude, the aircraft levels off

and decelerates to 250 kt (Segment 5). Fuel-optimal descents were determined by selecting the most fuel-efficient Mach/CAS descent combination for a given metering fix RTA (or time-to-fly).

2.3. Speed Strategy Fuelburn

Time-to-fly and fuelburn contours were interpolated from simulated flight data over a spectrum of Mach/CAS combinations that satisfied a range of constrained descent profiles. These profiles were characterized by the five-step nominal approach trajectory of Figure 5. Constant-time (RTA) and constant-fuelburn contours were then used to generate plots of user-preferred FMS and CTAS EDA descent speed profiles to meet a range of metering fix arrival times. The minimum fuel (fuel-optimal) descent Mach/CAS speed profiles were chosen to represent the user-preferred descent speeds assumed to be developed by the FMS.

This effort makes use of previous studies, which modeled and evaluated the fuelburn characteristics for two aircraft to compare descent fuel consumption under user-preferred FMS and CTAS EDA time-of-arrival control strategies. In each case, accurate aerodynamic and propulsion performance models were used to simulate aircraft trajectories and fuelburn estimates at two initial cruise speeds. The high-fidelity model results of two aircraft types were extrapolated fleet-wide using scaling factors based on aircraft performance characteristics.

High-Fidelity Aircraft Performance Simulations

In order to determine accurate fuelburn values for different RTAs, both MD-80 (MD8076) and B-747 (B74785) descents were simulated using a high-fidelity aircraft performance model. Photographs of these aircraft are shown in Figure 8.



Figure 8. Photographs of MD-80 and B-747 Aircraft

The high-fidelity model integrates accurate airframe and engine models with high-fidelity aircraft dynamics [20]. The model accurately simulates aircraft behavior by integrating the aircraft equations of motion. Aircraft are represented by a point mass model with pitch and turn dynamics. Point mass equations are used to represent the translational dynamics of the aircraft. Three degrees of freedom associated with aircraft position and an additional degree of freedom for roll orientation are used to provide realistic representation of the aircraft dynamics. Accurate aircraft dynamics, coupled with high-fidelity aerodynamic and propulsion models, were used to calculate the fuelburn data presented in this report.

Analysis of the user-preferred FMS and CTAS EDA speed control methods entailed simulating descent trajectories following the previously described descent speed strategies. In the determination of descent fuelburn consumption using the high-fidelity models, several thousand descents were simulated over a range of 150 nm. Simulations were performed using various Mach/CAS descent speed combinations for each aircraft, at two initial cruise speeds (maximum and nominal). The nominal speed case was used in this analysis. The fuelburn results are also dependent on assumed aircraft weight and meteorological conditions (wind, temperature).

The data collected for each fixed-range trajectory included fuelburn and time-to-fly for each Mach/CAS speed pair. Lines of constant time-to-fly and of constant fuelburn were extrapolated from this grid of data. Figure 9 illustrates sample contours of fixed time and fuelburn for a 564,000 lb B-747 aircraft flying a fixed range from 35,000 ft descending to 10,000 ft, assuming no wind and standard day conditions. The x-axis in each plot refers to the descent CAS (segment 4) of the descent speed strategy. The y-axis refers to the descent Mach speed (segment 3). Note that the Mach/CAS combination required to meet a given time-to-fly is not unique. Any operationally feasible Mach/CAS pair may be selected from a single contour to meet the specified time-of-arrival. Because of the speed, altitude and range tolerances on the simulation stopping point, there was a small amount of scatter in the data. Therefore, for each set of trajectories, the collected fuelburn and time-to-fly data were smoothed by surface fitting using polynomial functions of the Segment 3 descent Mach and Segment 4 descent CAS values. These smoothed time and fuel contours are apparent in Figure 9 and depicted as background in the plots that follow.

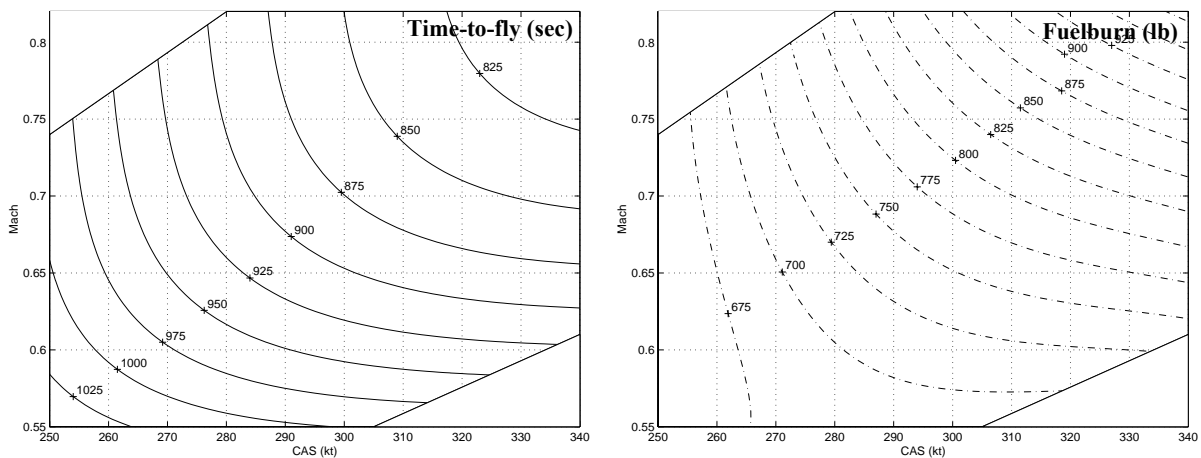


Figure 9. Time-to-Fly and Fuelburn Contours by Mach/CAS Descent Speed Pairs

Fuel-optimal user-preferred FMS Mach/CAS speed combinations were selected from the data (minimum fuel at each time-to-fly), while CTAS EDA speed strategy was determined by simulation of the aforementioned CTAS logic.

Figures 10a and 10b map all combinations of Mach (y-axis)/CAS (x-axis) descent pairs over a reasonable speed range for the two aircraft types. On each plot two sets of contours identify the fuelburn and time associated with each Mach/CAS speed profile, as solid and dashed lines, respectively. Locations of minimum fuel for each descent duration (time-to-fly) are marked with an asterisk. This curve is assumed to represent the hypothetical FMS performance. Square boxes are used to represent the CTAS EDA C=D speed combinations that are assumed to be issued to the aircraft without CTAS-FMS negotiation.

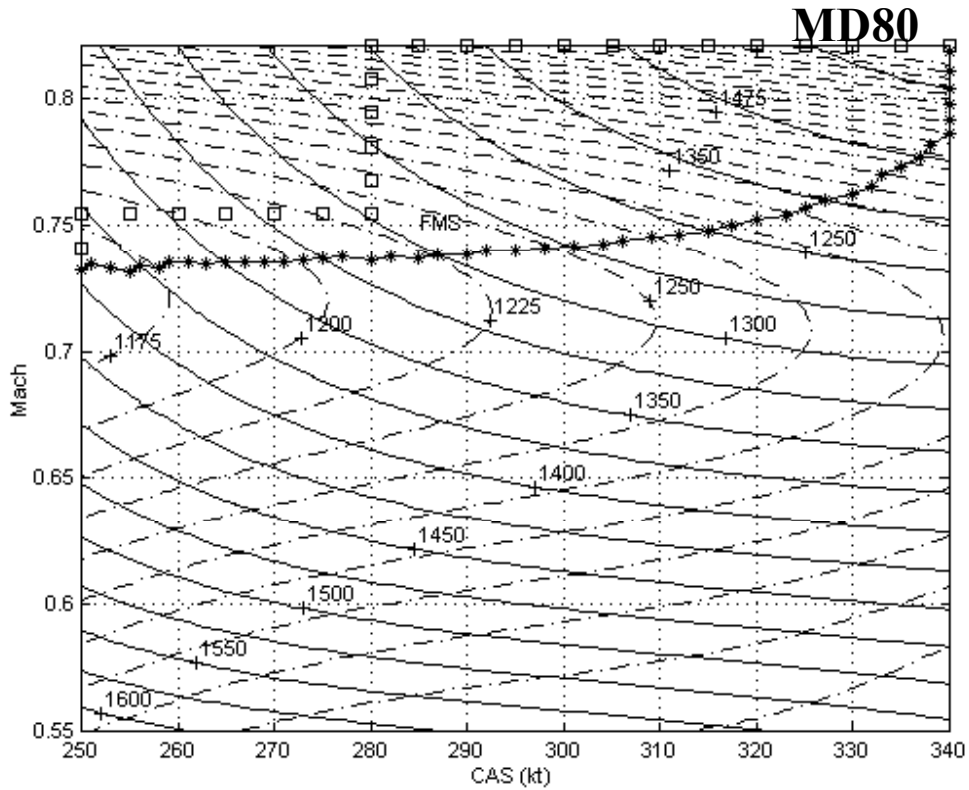


Figure 10a. Mach/CAS Plots for the MD-80 Aircraft

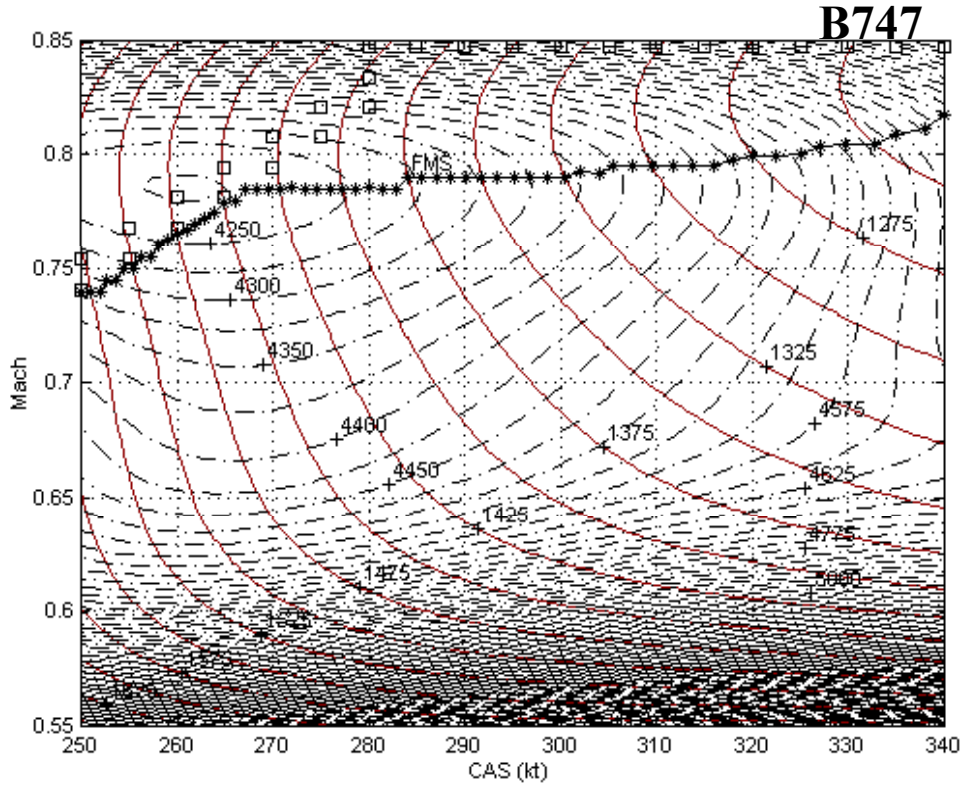


Figure 10b. Mach/CAS Plots for the B-747 Aircraft

When the fuelburn information of Figure 10 is plotted against descent duration or metering fix RTA, as in Figure 11, CTAS-FMS negotiation fuel savings can be estimated. Using these Fuel/RTA plots, the effect of different speed control strategies on fuelburn can be determined for a particular aircraft RTA.

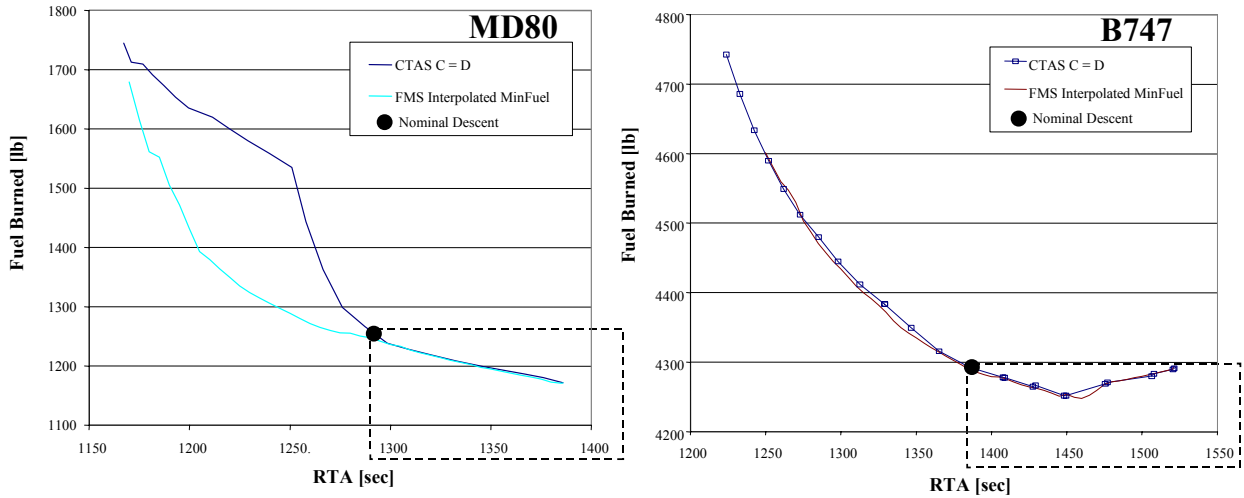


Figure 11. Fuel/RTA Plot for MD-80 and B-747 Aircraft

To determine the effect of speed control strategy on fuelburn for the metered DFW traffic, the information from Figure 11, Fuel-RTA plots, were transformed from RTA-based to delay-based values. To do so, nominal cruise Mach and descent CAS speeds were chosen for both aircraft based on airline operations manuals [21-22]. These speed choices, in turn, determined a nominal (or undelayed user-preferred) RTA. Table 2 shows the chosen speeds for both aircraft and the resulting nominal RTA and fuelburn for a descent from 35,000 to 10,000 ft over the simulation distance of 150 nm.

Table 2. Assumed Nominal (Undelayed) Descent Trajectory

Aircraft	Assumed Nominal Descent Speeds		Resulting Descent Characteristics	
	Cruise Mach	Descent CAS (kt)	RTA (sec)	Fuelburn (lb)
MD-80	0.76	280	1,294	1,248
B-747	0.85	280	1,385	4,291

Once determined, the nominal RTA was used to represent the zero delay point, as identified in Figure 11, with larger RTAs representing delayed operations. These portions of the Figure 11 plots (dashed boxes) are shown in Figure 12, with delay (relative to the nominal RTA) as the x-axis. Due to the fact that interpolation was used between data points to find potential fuel savings at particular delay times, the “perfect” FMS fuelburn may, in some places, be slightly greater than the CTAS EDA fuelburn value at a given delay. In subsequent use, all negative values were assumed to represent zero fuel savings. Note that Figure 12 shows that CTAS EDA is quite accurate in modeling minimum fuelburn descents for delayed flights. Figure 11 shows that significantly more CTAS-FMS speed negotiation savings would be expected when flights are expedited at a faster than nominal descent. Additionally, it should be noted that Figures 11 and 12 indicate that the maximum amount of delay that can be absorbed with speed control, given the assumed nominal descents, is on the order of 1-2 minutes. Other delay methods would be necessary to absorb additional delays.

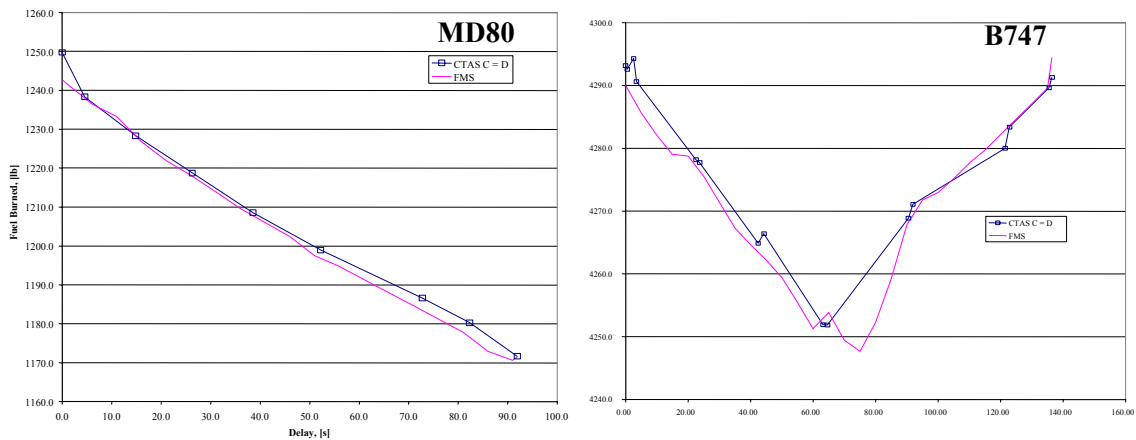


Figure 12. Fuelburn vs. Delay Plots for MD-80 and B-747 Aircraft

Fuel Scale Factors

To determine the per aircraft fuel savings, a factor was applied to the high-fidelity MD-80 and B-747 fuelburn results to reflect variances in aircraft performance across the fleet. This factor, referred to as the fuel scale factor (FSF), allowed the simulated results to cover a potentially large number of different aircraft types, based on Eurocontrol's Base of Aircraft Data (BADA) aircraft models [23].

The scaling of fuelburn between the high-fidelity MD-80 and B-747 aircraft models and the fleet-wide BADA aircraft models was done by comparing fuelburn rates for the aircraft during cruise operation. The assumption is that descents occur at or very near idle thrust conditions, and that the descent fuelburn should scale between aircraft models with the same order of accuracy as the cruise fuelburn. Heavy aircraft were scaled relative to the B-747 aircraft, all others were scaled relative to the MD-80 aircraft

The BADA aircraft performance models are based on a Total Energy Model (TEM). In this type of approach, aircraft are modeled as point masses, and the rate of work of the forces acting on the aircraft is equated to the rate of change of the aircraft's potential and kinetic energy. Literally dozens of coefficients are used to determine each of the explicit aircraft models. Typical weight and speed ranges and other operating values are supplied with each of the aircraft models. For this analysis, four parameters were manipulated to determine nominal fuelburn for each of the models: route length, altitude, aircraft weight, and aircraft speed. Common route length of approximately 250 nm of steady-level flight was modeled. Flights were simulated at each aircraft's nominal weight, at its nominal cruise Mach, and at its maximum operational altitude, as supplied in the BADA performance files. However, all of the aircraft models were not able to operate at their maximum altitude using the cruise Mach and nominal weight. For these aircraft, the altitude was lowered in 1,000 ft increments as needed. If the models didn't function properly at significantly lower altitudes, a combination of lower operational altitude and lower cruise Mach number was used. The resulting parameter assumptions for each aircraft type are identified in Appendix A. Altitudes and cruise Mach numbers that differ from the target BADA-supplied values are highlighted.

Some aircraft from the DFW trajectory data set had aircraft identifiers that were either "unknown" or non-standard ICAO/BADA identifiers (71 cases). In these cases, a fuel scale factor of 1 was used. This had the effect of modeling the unidentified, heavy aircraft as B-747s and other unidentified aircraft as MD-80s.

3. Potential EDX Fuel Benefits

The simulated potential fuelburn savings of implementing CTAS-FMS trajectory negotiation to DFW delayed arrivals are presented in Table 3. It is estimated that for the 1,047 arrival operations occurring on the simulated DFW day, CTAS TMA would have delayed 70 percent of these arrival flights with an average of 4 minutes for a daily total of 44.5 minutes of delay. If speed control with full data exchange was used to absorb as much of this delay as possible, a potential fuel savings of almost 2,000 lbs could be realized. This averages to nearly 3 lbs of fuel per delayed arrival operation, although the median is less than 1 lb, as shown in Figure 13. The resulting fuel benefits shown in Table 3 apply a conservative fuel cost of \$0.10 per lb to calculate daily and per operation savings at DFW.

Table 3. DFW Fuel Benefits

	Daily Delayed Arrivals	Average Savings Per Rush Arrival Operation
Daily Number of DFW Arrival Operations	732 (1)	NA
Daily TMA Delay	44.51 min	3.6 min/op
Daily Fuel Savings	1,991 lb	2.7 lbs/op
Daily Cost Savings (2)	\$199	\$0.27/op

(1) 70% of all modeled DFW arrivals were delayed.

(2) Assumes fuel cost of \$0.10 per lb.

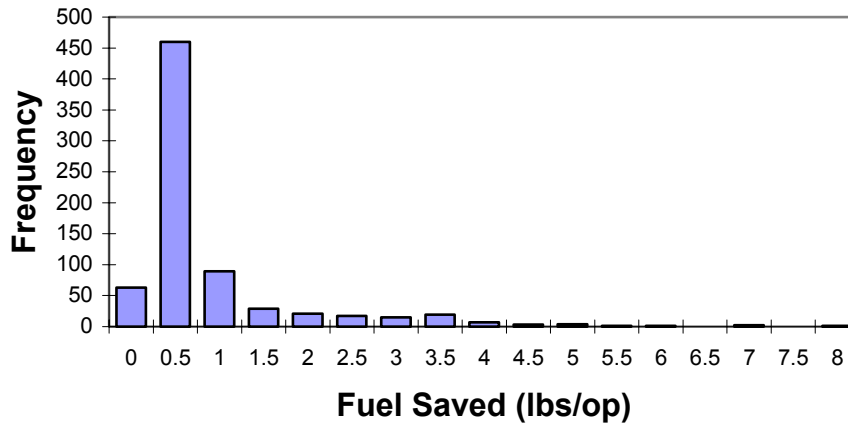


Figure 13. Fuel Savings per Operation

1996 NAS-wide Annual Savings

The simulated daily DFW savings can be extrapolated to an annual and NAS-wide level by accounting for the total number of 1996 delayed arrival operations at each facility. NAS benefits are calculated based on deployment in the en route airspace of 43 candidate airport sites. These CTAS EDA deployment airports were chosen to represent high-demand NAS airports, including FAA Free Flight Phase 1 (FFP1) and Phase 2 deployment locations.

The simple extrapolation used here employs Equation (1) to estimate benefits, as employed in other studies [12].

$$\text{Annual Savings} = (\text{Annual Ops}) \times (\text{Rush Arrivals}_{DFW}) \times (\text{Apt Factor}) \times (\text{Savings Per Interrupt}) \quad (1)$$

where: *Annual Ops* = Annual airport operations (00s) [24]

*Rush Arrivals*_{DFW} = DFW number of rush arrivals per 100 daily airport operations (Table 4)

Apt Factor = Factor accounting for local airport rush arrival frequency relative to DFW, based on FAA delay data (Table 5)

Savings Per Interrupt = Average cost savings per rush arrival (Table 4)

The DFW rush arrival rate and costs observed in the daily simulation and used in Equation (1) are summarized in Table 4.

Table 4. DFW Daily Simulation Interruption Rates and Costs

Parameter	Value
DFW Rush Arrival Rate (per 100 Airport ops)	30.4
Average Savings Per Interrupt	\$0.27/op

The rush arrival rates are adjusted by airport to account for variations in congestion at each facility. Airports with less overall delays are assumed to require disproportionately fewer arrival metering delay interruptions. Thus, airports with less demand-capacity congestion are assumed to delay fewer en route arrival aircraft to meet airport-scheduling constraints. An individual airport's assumed rush arrival rate is adjusted from the simulated DFW values (Table 4) based on the airport's delay rankings, using FAA delay data [25]. These data record delays at each airport in excess of 15 minutes in CY1996, including both arrivals and departures. This metric hides the significant number of smaller delays during an arrival rush period and includes delayed departures, making it a gross indicator of the airport's level of delayed arrival flights. Despite these limitations, this data provided a reasonable factor for extrapolating the detailed DFW traffic analyses to the 37-NAS airports. To do so, the NAS airports were broken into five delay categories, according to the criteria shown in Table 5. Engineering judgement was used to assign each category a rush arrival rate relative to DFW. Simulated rates of 130%, 115%, 100%, 80%, and 60% for airport delay classes 1, 2, 3, 4, and 5 were used. The annual airport operations [24], FAA delay data [25], associated delay category and rush arrival rate, by airport are shown in Table 6.

Table 5. Rush Arrival Rate Criteria

Category No.	CY1996 (1) Delays > 15 minutes Per 1000 Airport Ops	Proportion of DFW (category 3) Rush Arrival Rate	Rush Arrival Rate (Rush Arrivals Per 100 Airport Ops)
1	>35	130%	39.46
2	25-35	115%	34.91
3	15-25	100%	30.35 (2)
4	5-15	80%	24.28
5	<5	60%	18.21

(1) FAA CY1996 Delay Data [25], as shown in Table 6.

(2) DFW Rush Arrival Rate per simulation [13], in Table 4.

The estimated annual savings by airport are shown in Table 6 and plotted graphically in Figure 14. The large hub airports, ORD, DFW, ATL, and LAX, showed savings of over \$60,000 per year. Benefits at all 37 airports, representing NAS-wide deployment, totaled over \$1.1M annually. These results assume that EDA can compute speed changes to increment the metering fix RTA by 5 or 10 sec, and that the associated speed changes incorporating FMS speed preferences, are provided by the controller in an accurate and timely way. It should be noted that this analysis assumes underlying calibration of EDA trajectory prediction with the exchange of aircraft wind/temperature and aircraft weight. It is unknown how much additional benefit would result from these data exchanges. Additionally, this analysis could be used to improve the assumed CTAS EDA speed strategies.

Table 6. User-Preferred Descent Speed Profile Annual Savings

Airport	Annual Airport Ops (000s)	Apt Delay Delays/Category	Rush Arrival Rate	Annual Cost Saving (\$000s, 1998)	
Atlanta (ATL)	773	23.88	3	30.4	63.3
Nashville (BNA)	226	1.36	5	18.2	7.9
Boston (BOS)	463	0.73	2	18.2	11.1
Bradley (BDL)	161	26.37	5	34.9	43.6
Baltimore (BWI)	270	3.67	5	18.2	13.3
Cleveland (CLE)	291	4.68	5	18.2	14.3
Charlotte (CLT)	457	6.55	4	24.3	30.0
Cincinnati (CVG)	394	10.38	4	24.3	25.8
Washington National (DCA)	310	6.53	4	24.3	20.3
Denver (DEN)	454	1.90	5	18.2	22.3
Dallas – Ft. Worth (DFW)	870	19.59	3	30.4	71.3
Detroit (DTW)	531	9.10	4	24.3	34.8
Newark (EWR)	443	65.25	1	39.5	47.2
Ft. Lauderdale (FLL)	236	1.53	5	18.2	11.6
Houston Hobby (HOU)	252	2.57	5	18.2	12.4
Washington Dulles (IAD)	330	6.81	4	24.3	21.7
Houston–Intercontinental (IAH)	392	11.45	4	24.3	25.7
N.Y. Kennedy (JFK)	361	29.53	2	34.9	34.0
Las Vegas (LAS)	480	3.68	5	18.2	23.6
Los Angeles (LAX)	764	24.13	3	30.4	62.6
N.Y. LaGuardia (LGA)	343	46.22	1	39.5	36.5
Orlando (MCO)	342	4.59	5	18.2	16.8
Chicago Midway (MDW)	254	6.70	4	24.3	16.7
Memphis (MEM)	364	NA	5	18.2	17.9
Miami (MIA)	546	6.79	4	24.3	35.8
Minneapolis (MSP)	484	9.29	4	24.3	31.7
Oakland (OAK)	516	NA	5	18.2	25.4
Chicago O’Hare (ORD)	909	34.46	2	34.9	85.7
Portland (PDX)	306	2.41	5	18.2	15.0
Philadelphia (PHL)	406	17.95	3	30.4	33.3
Phoenix (PHX)	544	7.25	4	24.3	35.7
Pittsburgh (PIT)	447	6.60	4	24.3	29.3
San Diego (SAN)	244	3.31	5	18.2	12.0
Seattle (SEA)	398	6.37	4	24.3	26.1
San Francisco (SFO)	442	56.57	1	39.5	47.1
Salt Lake City (SLC)	374	3.53	5	18.2	18.4
St. Louis (STL)	<u>517</u>	<u>34.04</u>	<u>2</u>	<u>34.9</u>	<u>48.8</u>
37-Airport Total	---	---	---	---	1,129

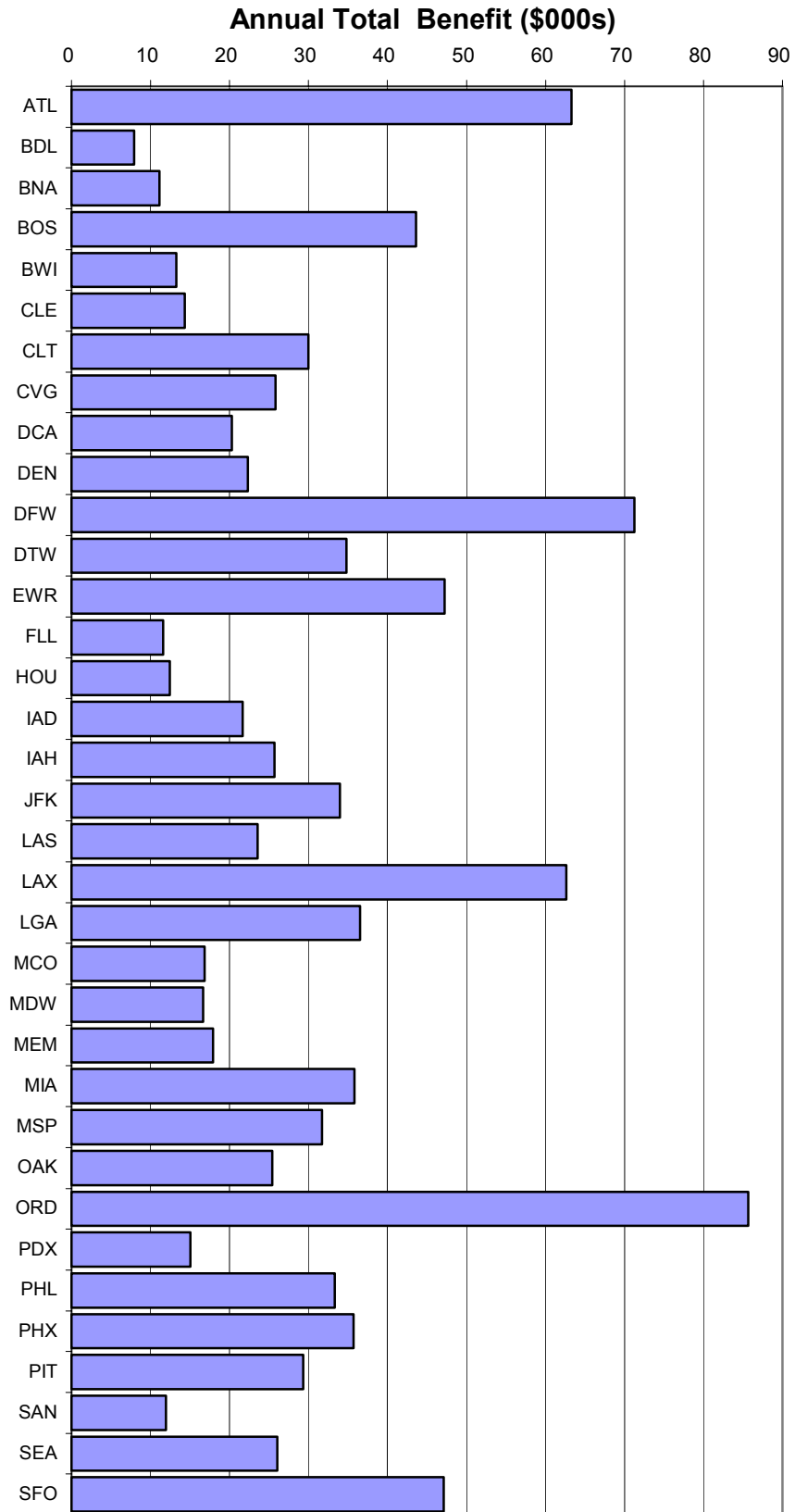


Figure 14. User-Preferred Descent Speed Profile Annual Savings

An examination was made of the effect of moving the assumed nominal descent speed profile of the MD-80 to a different Mach/CAS pair. The values of 0.8Mach/280kt CAS (replacing 0.76/280) were used as an alternate. Since fuel consumption of most aircraft types were scaled relative to the MD-80, a shift in the speed profile and associated fuelburn has an impact. The fuelburn versus RTA plot of Figure 11 compares the differences in fuelburn for the user-preferred FMS and CTAS EDA curves from Figure 10. The dotted rectangle represents the region where the aircraft would be slowed down from the nominal operating point to absorb delay. With the nominal point set at 0.76M/280kt, the user-preferred FMS and CTAS EDA curves are very similar showing negligible fuel savings between the two.

Looking at Figure 11 using the modified 0.8/280 nominal speed profile, puts the nominal operating point at an RTA of 1,265 seconds on the upper curve and re-positions the dotted box further up and to the left. At this new operating point small delays of 30 seconds or less (RTAs of 1,295 seconds or less), which represent 15 percent of all delays, save up to 130 lbs per flight when using the downlinked FMS profile. For delays larger than 30 seconds, the savings are again negligible (i.e., FMS and CTAS EDA lines converge). Under this basis, a rough estimate of the savings was found to be \$550 per day, an increase of about \$350.

However, since most of the modified nominal point benefits occur below 30 seconds, the feasibility of realizing these benefits is questionable. Indeed, it is unclear whether controllers could be sensitized or would negotiate with the aircraft via datalink, for delays less than 15 seconds. Furthermore, the nature of the fuelburn differences between the CTAS EDA and user-preferred FMS curves of Figure 11 is peculiar to the nominal CTAS speed profile used to mechanize different RTAs for delay absorption for the MD-80, as taken from Figure 10. This MD-80 curve could be brought closer to the user-preferred FMS curve by changing the parameters used to characterize this profile within CTAS. Thus, these results are an artifact of this particular CTAS speed profile.

If potential savings were limited to flights which absorbed delays over 15 seconds (6 percent of all delays) the resulting savings are much closer to the original \$200 per day estimate. In sum, this exercise identified a fuelburn sensitivity to changes in MD-80 nominal descent speeds, but the potential gain was insufficient to justify higher potential benefit numbers for this EDX mechanism.

Conclusions and Recommendations

This report has identified the potential benefits of replacing CTAS EDA descent speed profiles with user-preferred FMS speed profiles for delayed arrival operations. The FMS downlink of the user-preferred altitude-speed profile to meet an arrival fix crossing time (RTA) allows more fuel-efficient descents while adhering to airport capacity restrictions. The downlinked preferences would enhance CTAS EDA-calculated altitude-speed profiles, saving aircraft fuel in descent. Relative to the CTAS EDA Baseline, it was found that CTAS-FMS descent speed negotiation saved an average of 3 lbs of fuel or \$0.27 per rush arrival, with total savings of \$1.1M annually assuming NAS-wide deployment at 37-airports. This does not include the benefits of wind/temperature and aircraft weight data exchange, assumed to be part of the baseline.

To achieve these benefits, it is assumed that EDA can compute speed changes to increment the metering fix RTA by 5 or 10 sec, and that the associated speed changes incorporating FMS speed preferences, are provided by the controller in an accurate and timely way. Additionally, these benefits require a RTA-capable FMS equipage and time-critical data link to uplink a metering fix RTA and downlink the FMS preferred speed profile.

The following are recommendations for refining the analysis:

- **Improve Fleet-wide Fuelburn Extrapolation** - For this study, only two high-fidelity aircraft models were available to model fuelburn. In order to make a fleet-wide extrapolation of the potential benefits, lower fidelity aircraft models were used to obtain fuelburn rates for the remaining aircraft, scaled to the higher-fidelity MD-80 and B-747 rates. To obtain more accurate fleet-wide fuelburn benefit estimates, more accurate fuelburn models that are representative of the variance of aircraft operating in the NAS should be used.
- **Investigate Sensitivity of Assumed Basic Data Exchange** – This analysis assumed that both the CTAS EDA and User-preferred FMS cases shared accurate weight and meteorological forecasts (wind, air temperature). Actual results may be affected by errors in aircraft data, atmospheric data or trajectory prediction accuracy. A sensitivity study could evaluate the degradation of the CTAS EDA and User-preferred FMS speed profiles under less ideal conditions.
- **Improve User-Preferred (FMS) Strategy Modeling** –User-preferred FMS descent speed preferences were modeled as the minimum-fuel (fuel-optimal) speed profile for a given arrival metering fix RTA. A more realistic model would incorporate existing FMS RTA trajectory modeling algorithms and account for operational constraints in choosing Mach/CAS profiles.
- **Verify Nominal Descent Speed Profile** – The resulting benefit estimate from this analysis is highly sensitive to the choice of nominal descent speed profiles. As shown in the sensitivity analysis. Field data analysis supported by discussions with airlines is recommended to confirm the choice of nominal speed profiles used in the analysis

Appendix A Fuel Scale Factor Assumptions

The following aircraft parameters were used with BADA [23] aircraft models to determine the fleet-wide Fuel Scale Factors.

Table A-1. Fuel Scale Factor Assumptions

Aircraft Type (ICAO)	Initial Weight (lb)	Weight Class	Mach	Altitude (ft)	Fuel Scale Factor
A300	275575	H	0.78	38000	0.5140
A310	264552	H	0.80	41000	0.4025
A320	136685	L	0.78	39000	0.8303
A330	352736	H	0.80	41000	0.4596
A340	440920	H	0.80	40000	0.6303
ATP	44092	L	0.40	21000	0.3290
A7R	33069	S	0.45	25000	0.2688
B707	220460	H	0.80	42000	0.5297
B727	163140	L	0.82	33000	1.4941
B73A	101412	L	0.72	37000	0.8532
B73B	119048	L	0.74	37000	0.8649
B73C	136906	L	0.79	43000	1.1480
B74A	617288	H	0.82	36000	1
B74B	661380	H	0.85	39000	1.0615
B757	209437	H	0.78	39000	0.3290
B767	330690	H	0.80	39000	0.4508
B777	465171	H	0.84	43100	0.7198
BA11	69886	L	0.72	35000	0.5697
BA46	79366	L	0.70	31000	0.8093
BE20	11010	S	0.48	32000	0.0538
BE99	9039	S	0.35	15000	0.1417
BE9L	8025	S	0.40	31000	0.1076
CL30	129983	L	0.50	30000	1.4601
CL60	88184	L	0.38	30000	0.6522
C421	6261	S	0.33	18500	0.1217
C550	13228	S	0.63	38000	0.2382
C560	13977	S	0.73	45000	0.2011
CARJ	46297	L	0.74	38000	0.3569
CL60	34061	L	0.77	41000	0.2541
D228	12346	S	0.34	29600	0.3082
D328	26455	S	0.59	32800	0.2596
DC10	374782	H	0.82	39000	0.5640
DC8	242506	H	0.80	42000	0.3149

Aircraft Type (ICAO)	Initial Weight (lb)	Weight Class	Mach	Altitude (ft)	Fuel Scale Factor
DC9	100089	L	0.80	35000	0.9943
DHC8	37478	L	0.45	25000	0.2065
E120	22046	S	0.47	32000	0.1735
F100	83775	L	0.70	35000	0.6606
F27	37478	L	0.37	20000	0.3972
F28	52910	L	0.70	35000	0.4969
F50	39683	L	0.44	25000	0.3261
F70	74956	L	0.70	37000	0.6218
F900	33951	L	0.80	44000	0.2607
FA10	15983	S	0.75	45000	0.1510
FA20	22046	S	0.76	42000	0.3128
FA50	33069	S	0.75	49000	0.2540
H25B	18001	S	0.75	41000	0.3433
J5TA	13669	S	0.41	25000	0.1681
J5TB	19841	S	0.42	26000	0.1924
L101	340611	H	0.82	40000	0.5160
LJ35	14991	S	0.77	38000	0.1959
MD11	501106	H	0.83	37000	0.7604
MD80	134922	L	0.76	37000	1
MU2	8988	S	0.57	28000	0.1126
P31T	7981	S	0.44	29000	0.1146
PA27	4806	S	0.50	10000	0.0659
PA28	2326	S	0.18	10000	0.0157
PA31	5489	S	0.33	20000	0.1284
PA34	4564	S	0.34	15000	0.1268
PA42	9101	S	0.46	33000	0.1182
SB20	44092	L	0.62	31000	0.3745
SF34	22046	S	0.45	31000	0.3367
SH36	24912	S	0.33	20000	0.2323
SW3	10582	S	0.52	31000	0.1371
T134	92593	L	0.78	37000	0.7185
T154	187391	L	0.80	41000	1.5321
TRIN	2943	S	0.35	8000	0.0302

Note: Heavy aircraft scaled relative to B-747 fuelburn rates, all others scaled relative to MD-80 fuelburn rates (lbs/nm)

Acronyms

ARTCC	Air Route Traffic Control Center
ATL	Atlanta Hartsfield International Airport
ATM	Air Traffic Management
B-747	Boeing Co. 747- Aircraft
BADA	Eurocontrol Base of Aircraft Data
BNA	Nashville International Airport
BOS	Boston Logan International Airport
BWI	Baltimore-Washington International Airport
C=D	CTAS Cruise Equals Descent Speed Strategy
C→D	CTAS Cruise then Descent Speed Strategy
CAS	Calibrated Airspeed
Center	Air Route Traffic Control Center (ARTCC)
CLE	Cleveland Hopkins International Airport
CLT	Charlotte-Douglas International Airport
CTAS	Center/TRACON Automation System
CVG	Cincinnati/Northern Kentucky International Airport
D→C	CTAS Descent then Cruise Speed Strategy
DCA	Washington National Airport
DEN	Denver International Airport
DFW	Dallas-Ft. Worth International Airport
DSR	Display System Replacement
DTW	Detroit International Airport
EDA	CTAS En Route/Descent Advisor
EWR	Newark International Airport
FAA	Federal Aviation Administration
FANG	FAA's FMS-ATM Next Generation Program

FLL	Ft. Lauderdale-Hollywood International Airport
ft	Feet
FMS	Flight Management System
FSF	Fuel Scale Factor
HOU	Houston Hobby International Airport
IAD	Washington Dulles International Airport
IAH	Houston–Intercontinental Airport
ICAO	International Civil Aviation Organization
JFK	N.Y. Kennedy International Airport
kt	Knot, Nautical Miles Per Hour
LAS	Las Vegas McCarran International Airport
LAX	Los Angeles International Airport
LGA	N.Y. LaGuardia Airport
MCO	Orlando International Airport
MD-80	McDonnell Douglas Corp. MD-80 Aircraft
MDW	Chicago Midway Airport
MEM	Memphis International Airport
MF	Metering Fix
MIA	Miami International Airport
MSP	Minneapolis-St. Paul International Airport
nm	Nautical Mile
NAS	National Airspace System
NASA	National Aeronautics and Space Administration
OAK	Oakland International Airport
ORD	Chicago O’Hare International Airport
PDX	Portland International Airport
PHL	Philadelphia International Airport

PIT	Greater Pittsburgh International Airport
ROM	Rough Order of Magnitude
RTA	Required Time-of-Arrival
SAN	San Diego International Airport
SEA	Seattle–Tacoma International Airport
SFO	San Francisco International Airport
SID	Standard Instrument Departure
SRC	Systems Resources Corporation
STA	Scheduled Time-of-Arrival
STAR	Standard Terminal Arrival Route
TAS	True Airspeed
TEM	Total Energy Model
TMA	CTAS Traffic Management Advisor
TOD	Top of Descent
TRACON	Terminal Radar Approach Control
ZFW	Ft. Worth Air Route Traffic Control Center

References

- [1] Erzberger, H., "Design Principles and Algorithms for Automated ATM," AGARD Lecture Series No. 200 on Knowledge-based Functions in Aerospace Systems, Germany. (November 1995)
- [2] Green, S.M., and Vivona, R., "En route Descent Advisor (EDA) Concept," Advanced Air Transportation Technologies (AATT) Project Milestone 5.10 Report, NASA Ames Research Center. (September 1999)
- [3] Green, S., Goka, T., Williams, D., "Enabling User Preferences through Data Exchange," AIAA GN&C Conference, AIAA-97-3682. (August 1997)
- [4] Williams, D.H., and Green, S.M., "Piloted Simulation of an Air-Ground Profile Negotiation Process in a Time-Based Air Traffic Control Environment," NASA TM-107748. (April 1993)
- [5] Green, S.M., Williams, D.H., and den Braven, W., "Development and Evaluation of a Profile Negotiation Process for Integrating Aircraft and Air Traffic Control Automation," NASA TM-4360. (April 1993)
- [6] FMS-ATM Next Generation (FANG) Team, "FANG Operational Concept," FAA and Boeing Commercial Airplane Group CRDA 93-CRDA-0034. (February 1996)
- [7] Anon, "Study of the Acquisition of Data from Aircraft Operators to Aid Trajectory Prediction Calculation," Eurocontrol, EEC Note No. 18/98. (September 1998)
- [8] FMS-ATM Next Generation (FANG) Team, "FMS-ATM Next Generation (FANG) Required Capabilities," DOT/FAA/AND-98-14, FAA. (November 1998)
- [9] Weidner, T., Schleicher, D., Coppenbarger, R., "NASA/FAA En Route Data Exchange (EDX) Phase 2 Field Evaluation Project Plan," Seagull Technology, TR99185.04-01. (February 2000)
- [10] Tysen Mueller Tara Weidner "Enhanced Surveillance, Data Link Study Plan," Seagull Technology TR184.01-01. (June 2000)
- [11] FAA Aeronautical Data Link Program (ADL) AND-370 website <http://38.243.118.34/>
- [12] Weidner, T., Mueller, T., "Benefits Assessment Compilation for En Route Data Exchange (EDX)," Seagull Technology TR00188.27-01f. (December 2000)
- [13] Weidner, T., Davidson, T.G., Dorsky, S., "En Route Descent Advisor (EDA) and En Route Data Exchange (EDX) ATM Interruption Benefits," Seagull Technology, TR 98188.26-01f, NASA TO26. (December 2000)
- [14] Weidner, T., Green, S., "Modeling ATM Automation Metering Conformance Benefits," 3rd USA/Europe Air Traffic Management R&D Seminar, forthcoming. (July 2000)
- [15] Davidson, T.G., Birtcil, L., "Comparison of Fuel Optimal, CTAS and FMS Time-of-Arrival Control Strategies for MD-80 Aircraft Trajectories," Seagull Technology, TR178-02. (Sept 1998)
- [16] Davidson, T.G., Birtcil, L., "Comparison of Fuel Optimal, CTAS and FMS Time-of-Arrival Control Strategies for B-747 Aircraft Trajectories," Seagull Technology, TR178-03 (Sept 1998)
- [17] Davidson, T.G., Birtcil, L., Green, S., "Comparison of CTAS/EDA and FMS Time-of-Arrival Control Strategies," AIAA GN&C Conference, AIAA99-4230. (August 1999)
- [18] CSSI Inc., "Traffic Demand Scenarios" computer data files. (September 1998)
- [19] Swensen, H., et al, "Design & Operational Evaluation of the Traffic Management Advisor at the Fort Worth ARTCC," 1st USA/Europe ATM R&D Seminar, France. (June 1997)
- [20] Mukai, C., "Design and Analysis of Aircraft Dynamics Models for the ATC Simulation at NASA Ames Research Center," TM92119-02, Seagull Technology, Inc., Los Gatos, CA. (March 1992)
- [21] MD-80, American Airlines Operation Engineering. (1998)
- [22] United 747 Flight Manual, p.816, Operating Speeds. (January 1988)
- [23] Eurocontrol Experimental Centre, "User Manual for the Base of Aircraft Data (BADA) Revision 3.1," EED Note No. 23/97, Eurocontrol. (October 1998)

- [24] FAA, "1997 Terminal Area Forecast (TAF) System," Office of Aviation Policy and Plans, FAA APO Home Page, Internet WWW Site. (October 1998)
- [25] FAA, "1997 Aviation Capacity Enhancement Plan," Office of System Capacity. (Dec 1997)